Pergamon

Int. J. Heat Mass Transfer. Vol. 40, No. 13, pp. 3089–3104, 1997
© 1997 Elsevier Science Ltd. All rights reserved
Printed in Great Britain
0017–9310/97 $17.00 + 0.00

PII: S0017–9310(96)00361–4

The effects of chaotic advection on heat transfer

A. MOKRANI, C. CASTELAIN and H. PEERHOSSAINI

Thermofluids and Complex Flows Research Group, Laboratoire de Thermocinétique, URA CNRS 869, Université de Nantes, ISITEM, La Chantrerie CP 3023, F44087 NANTES Cedex 03, France

(*Received* 12 *February* 1996 *and in final form* 10 *October* 1996)

Abstract—The objective of this study is to characterize a new heating process in fluids, chaotic advection. The main mechanism generating this flow is the production of spatially chaotic trajectories in an alternating Dean flow. The present work examines the effects of chaotic advection on heat transfer at low Reynolds numbers. In order to assess the enhancement of heat transfer by chaotic advection, a helical heat exchanger and a chaotic heat exchanger (both of shell-and-tube type) of the same heat-transfer surface area and the same tube length were tested. The coils were assembled from 90° bends, and the chaotic coil was produced merely by turning each bend at a $\pm 90°$ angle with respect to the previous one. Experiments were performed for Reynolds numbers ranging from 60 to 200. Temperature profiles measured in the cross-section of the coils show that chaotic advection substantially homogenizes and enhances heating. Moreover, it is shown that the homogeneity of heating in chaotic flow is almost independent of the Reynolds number. Parallel to the temperature profiles measurements, axial velocity profiles were measured by laser Doppler velocimetry at the exit from the coils and used to characterize the flow in the isothermal regime and compare the temperature profiles to the velocity profiles. Global heat-transfer measurements show that the chaotic heat exchanger is more efficient than the helical one, with an efficiency enhancement between 13 and 27%.
© 1997 Elsevier Science Ltd.

1. INTRODUCTION

The homogeneous heating of delicate and viscous fluids is a difficult operation. Conventional techniques are based either on increasing the heat-transfer surface area or augmenting mixing in the fluid. The former technique incurs extra pumping costs, since the fluid experiences higher shear stress due to the additional non-slip surfaces. Good fluid mixing can be achieved in turbulent flows, but once again the drawback is the higher shear stress, which increases the pressure drop and pumping cost. In addition, it becomes difficult to enhance heat transfer in cases where turbulence cannot be generated in the flow due to high viscosity.

Some delicate fluids (such as human blood or food liquids) contain long chains of molecules that can easily be damaged by shear stresses. Such products are usually heated by mixing them in laminar flow through helical coiled heat exchangers. The transverse motion developed in laminar flow through coiled tubes (the Dean roll-cells) transports cold particles from the center of the tube to the hot regions close to the wall. This mechanism enhances global heat transfer and is commonly used for this purpose [1]. Numerical and experimental studies with the helical geometry show that for the same heat-transfer surface area, the inner Nusselt number is greater than that in a straight tube [2–5]. It is also found that the relative enhancement of the Nusselt number is greater than the relative increase in head loss due to additional momentum transport in the transverse direction. In fact, there is global heat-transfer enhancement, but Raju and Rathna [6] showed that in helical coiled tubes the isotherms of temperature for different kinds of fluids (Newtonian, pseudoplastic or dilatant) contain segregated cold and hot regions. The Dean roll-cells divide the cross-section into two zones in each of which the isotherms form closed curves. Fluid particles inside the Dean roll-cells are prevented from approaching the hot walls; thus mixing is poor, giving rise to a heterogeneous temperature field.

Recent studies [7–9] present an alternative regime in laminar flow that has dispersive properties close to a turbulent regime. This phenomenon, called chaotic advection or Lagrangian turbulence, is analogous to temporal chaos in which a small number of degrees of freedom can cause chaotic evolution over time. In chaotic advection, the fluid-particle trajectories are chaotic and enhance mixing, consequently increasing heat transfer.

While temporal chaos has been the subject of many investigations, chaotic advection has been studied only recently. Aref [10] established an analogy between a two-dimensional flow and a conservative dynamical system. In a two-dimensional stationary incompressible flow, the stream function is independent of time and invariant for each particle; the system is integrable. The streamline equations define a Hamiltonian system of one degree of freedom. In two-dimensional incompressible nonstationary flows, the streamlines follow a Hamiltonian system dependent on time that is in general non-integrable; the particle trajectories can become chaotic.

Some ideal flows have been studied to verify the

NOMENCLATURE

a	mean curvature radius
C_p	specific heat
D	tube diameter
Dn	Dean number, $Re\sqrt{D/a}$
e	non-dimensional eccentricity
f	fanning friction factor
k	viscosity coefficient
L	development or attenuation distance
n	rate index
Pe	Péclet number
Q	flow rate
Re	Reynolds number, VD/v
t	time
T	temperature
u, v, w	instantaneous Eulerian velocity field
x, y, z	instantaneous position of a fluid particle in the plane (xy) and axial direction
V	mean velocity.

Greek symbols

δ	radius ratio, $D/2a$
ε	heat exchanger efficiency
ϕ	heat flux
γ	shear rate
μ	dynamic viscosity
v	kinematic viscosity, μ/ρ
ρ	fluid density
τ	shear stress
$\psi(x, y)$	stream function.

Subscripts

av	average
e	entrance
i	intake
max	maximum
min	minimum
o	exit
s	shell-side fluid
t	tube-side fluid.

existence of chaotic advection. Aref [10] modeled a cylindrical mixing tank equipped with two agitators moving continuously or alternately with periodic displacement. Chaiken *et al.* [11] looked at the Stokes flow between two eccentric cylinders rotating alternately. Jones and Aref [12] analyzed a pulsed source-sink system.

Ghosh *et al.* [13] used Stokes flow between eccentric counter-rotating cylinders to investigate the effect of slender recirculation region within the flow field on cross-stream heat or mass transfer. In this lubrification flow they limited their study to high Péclect number Pe where the enhancement is most pronounced. They found that enhancement over pure conduction varies as $e^{1/2}$ at infinite Pe, where e is the nondimensional eccentricity and $e^{1/2}$ is the characteristic width of the recirculation region. This enhancement decays at $Pe^{-1/2}$ from the asymptotic value. Time periodic forcing of the rotation of the cylinders caused a further enhancement of the cross-stream flux due to the generation of chaotic particle transport. A similar flow geometry, the annular region between two concentric, confocal ellipses, was examined by Saadjian *et al.* [14, 15]. They have shown that for steady counter-rotation of the two ellipses, the recirculation zones can lead to 80% heat transfer enhancement over pure conduction at high Péclect numbers. This enhancement can reach up to 100% if one of the ellipses follow an appropriate sinusoidal modulation of the angular velocity.

In three-dimensional flow, chaotic regime does not even require a time-dependent system, since stationary three-dimensional flows are equivalent to two-dimensional flows depend on time (as can be observed by replacing one of the coordinates by a fictitious time). The necessary conditions for the existence of three-dimensional stationary flow with chaotic streamlines have been addressed by Arnold [16], who gave an example with the triply periodic solution of the Euler equation (ABC flow). Though this flow cannot be reproduced in laboratory, several designs suggested for using chaotic mixing in practical devices capture its essential features. One is the partitioned pipe mixer of Khakhar *et al.* [17], in which a central partition and rotation of the pipe produce chaotic trajectories. The other is an alternating sequence of bends [7, 18]. The former authors showed numerically that mixing can be enhanced by inserting a geometrical perturbation in the laminar flow. This perturbation is achieved by merely shifting each bend by an angle χ between 0 and 90°. The resulting twisted-duct geometry produces laminar chaotic pathlines of particles flowing inside the duct. Mixing is much more efficient in this case than in the helical coil.

Le Guer *et al.* [19] also studied the hydrodynamics of the flow in twisted bends. Their experimental results show that the flow produces a horseshoe map and pathlines are sensitive to the initial conditions. It has also been demonstrated that the flow produces very complex stretching and folding patterns in the material lines. In the zones where chaotic flow prevails, an exponential stretching rate is observed. It is well known that this behavior indicates that particle pathlines are chaotic [20]. Comparison of the variance of axial and transverse distribution of fly-time in the system showed that the increase due to the chaotic advection of the transverse variance is at least one order of magnitude greater than the decrease in the

variance of axial dispersion. Therefore, though from the Eulerian point of view the flow is locally a "regular" Dean flow, an important modification of the flow topology has occurred. Peerhossaini *et al.* [9] designed a heat exchanger based on chaotic advection in order to apply this new concept.

The aim of the present study is to examine the effect of chaotic advection on heat transfer. Thus, we compare two kinds of heat exchangers: a helical–coil heat exchanger and a twisted pipe coil that generates chaotic advection (hereafter called the chaotic coil). The same bends are used to construct both the chaotic and the helical coils: they are assembled in one way to form a helical coil and in another way to produce chaotic pathlines of the fluid particles flowing inside the tubes. Thus the two coils have the same heat-transfer surface area.

Our heat exchanger consists of the coils described above immersed (one at a time) in a polypropylene cubic shell. The secondary hot fluid (water) flows in the shell side whereas the primary cold fluid flows in the tube side. Our primary fluid is a non-Newtonian solution of carboxymethyl cellulose (CMC), one of the model fluids frequently used in food engineering. Experiments were performed for Reynolds numbers between 60 and 200.

Temperature profiles were measured at the exit of the coil in both configurations and velocity profiles were measured at the same positions in the isothermal case. In a second experiment, we measured heat-exchanger efficiency using the two coils so as to assess efficiency enhancement by chaotic advection.

The remainder of the paper is organized as follows. Section 2 gives a brief introduction to Dean flow as a base line for the production of chaotic pathlines in twisted bends. The experimental facility is described in Section 3. Section 4 is devoted to the procedure and experimental results, and Section 5 contains some concluding remarks.

2. DESCRIPTION OF THE BASIC FLOW

The focus of this work is the flow in a twisted pipe that is an assembly of 90° bends. This section gives a brief description of the flow in curved channels and of the modifications arising in the flow due to the switch in curvature plane of the bends.

2.1. *Dean flow*

The flow in the tube side of the heat exchangers under study here is that through a succession of bends: the basic flow is thus the flow in a curved duct. In laminar flow through a curved duct, centrifugal forces give rise to a secondary flow that consists of a pair of counter-rotating roll-cells. These roll-cells are known as Dean roll-cells after W. R. Dean [21, 22], who developed a theory of this secondary flow, following the observations of Eustice [23]; we thus call the flow through a curved duct "Dean flow". For higher Dean numbers, a centrifugal instability appears close to the outer concave wall of the tube and generates another pair of counter-rotating vortices known as Dean vortices.

It is important to distinguish between Dean vortices and Dean roll-cells. The main difference is the mechanism that gives rise to the two phenomena. Dean roll-cells are present even at the lowest Dean numbers and are due to the imbalance between centrifugal and viscous forces (similar to a box with differentially heated side walls). Dean vortices, on the other hand, are due to an instability phenomenon that appears only after an instability threshold is crossed (similar to Rayleigh–Bénard convection). Figure 1 shows two typical flows in curved ducts. The first one occurs at lower Dean numbers; it consists of Dean roll-cells only. The second one appears once the critical Dean number is achieved and includes Dean roll-cells and Dean vortices. As shown in Fig. 1, the other major difference is the space domain in which the cellular structures appear. Dean roll-cells occupy almost the whole cross-section, while Dean vortices occupy only a small part of it. The roll-cells are larger than the vortices. More detailed studies of the hydrodynamics of Dean flow are reported in Berger *et al.* [24], Bara *et al.* [25] and Le Guer *et al.* [19].

The Dean number is a nondimensional number that characterizes the flow in curved channels. It represents the ratio of centrifugal force to viscous and inertial forces and is defined as

$$Dn = Re\sqrt{\frac{D}{a}} \tag{1}$$

where a is the mean curvature radius.

2.2. *Fluid particle pathlines in twisted pipe flow*

In the Lagrangian representation of fluid motion, one searches for the trajectories of particles by formulating the velocity field as

$$\frac{\mathrm{d}x}{\mathrm{d}t} = u(x, y, z, t)$$

$$\frac{\mathrm{d}y}{\mathrm{d}t} = v(x, y, z, t)$$

$$\frac{\mathrm{d}z}{\mathrm{d}t} = w(x, y, z, t) \tag{2}$$

where (x, y, z) is the instantaneous position of a particle and (u, v, w) represents the instantaneous Eulerian velocity field. If the flow is steady, the independent variable t (time) can be replaced by the streamwise space variable z. This can be achieved by dividing the two first equations by the third, yielding a two-dimensional system.

In two-dimensional steady systems, the incompressibility conditions define a stream function $\psi(x, y)$. The problem can then be formulated as a Hamiltonian dynamical system:

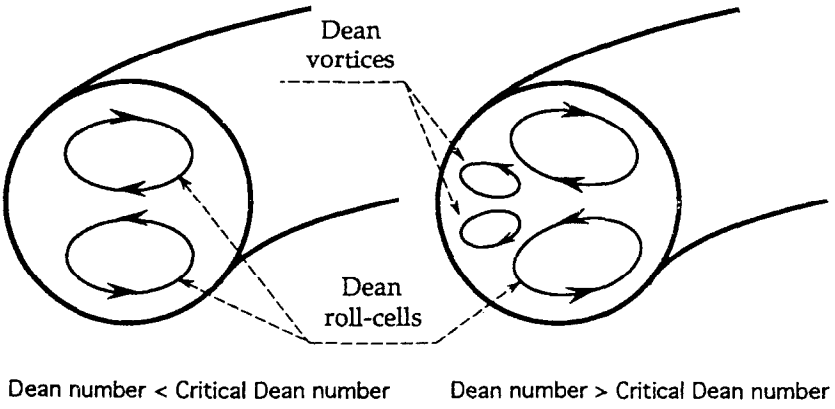

Fig. 1. Secondary flow in a curved duct.

$$\dot{x} = -\frac{\partial \psi}{\partial y} \quad \dot{y} = \frac{\partial \psi}{\partial x} \tag{3}$$

where the stream function ψ is the Hamiltonian. These equations describe a Hamiltonian system with one degree of freedom for which a solution in terms of regular functions is always possible. The fluid particle trajectories in this case are always non-chaotic. The analogy with Hamiltonian dynamics suggests that if the stream function is periodic in z, the laminar flow follows non-integrable Hamiltonian dynamics and gives rise to deterministic chaotic trajectories. In this sense the trajectories are complicated and sensitive to initial conditions. This phenomenon, which has been termed chaotic advection [10], enhances mixing.

Chaotic mixing becomes useful in practice in open flows, since many industrial devices involve flow in ducts. Chang and Sen [26] review previous work on the enhancement of heat transfer in fluids by chaotic mixing and describe several devices for practical applications. Here we study heat-transfer enhancement in one of these devices: the chaotic coil.

3. EXPERIMENTAL SETUP

Figure 2 is a photograph of the two coils tested in the chaotic and regular configuration. The coils immersed in the rectangular reservoir constitute two shell-and-tube heat exchangers, one helical and the other chaotic. A primary concern in the coil design was the similarity of their external geometry, which affects the flow of the secondary fluid around the coils in the shell. The coils are assembled from bends and straight tubes. The bends are 90° curved tubes of circular cross-section made of stainless steel; the inner and outer diameters of their cross-section are 23 and 25 mm, respectively, and their mean radius of curvature is 126.5 mm. Each bend is separated from the next by a straight section that decouples roll-cell formation in the upstream bend from that in the downstream bend. The bends and straight tubes are assembled using special connections that introduce no discontinuities at the joints.

The chaotic coil, obtained merely by rotating each bend by 90° with respect to the neighboring bend, consists of 33 bends and 11 straight tubes of 80 mm each. The helical coil is an assembly of the same 33 bends and 16 straight tubes of 55 mm each. Thus the coils have the same heat-transfer surface area.

A schematic diagram of the heat exchanger is shown in Fig. 3. It consists of the coils described above immersed (one at time) in a polypropylene cubic shell. All faces of the shell are insulated with panels of expanded polystyrene 4 cm thick in order to minimize heat loss to the surrounding air.

Temperatures are measured by chromel–alumel thermocouples of 80 μm diameter located as shown in Fig. 3. Entrance and exit temperatures of the shell-side fluid are measured by the two thermocouples (3) and (4) fixed in the center of the tube cross-section. Two probes (1) and (2) allow measurement of the intake and exit temperature profiles of the tube-side fluid along the tube diameter by a micrometric displacement mechanism.

A heat exchanger test facility, the schematic diagram of which appears in Fig. 4, was designed to test the two heat exchangers. It is made of a primary cold loop and a secondary hot loop. The heat exchanger under test is shown in the center. The cold loop is designed to operate with different types of fluids, especially delicate non-Newtonian and very viscous fluids. It consists of an overhead reservoir (1) of 160 l capacity that damps the temperature fluctuations. The fluid is continuously mixed in the reservoir in order to homogenize its temperature. The cold fluid is pumped through the loop using a helical shaft pump (Moineau pump) (2). These pumps are widely used in food-processing industries because they exert a low shear stress on the fluid. The flow rate is controlled by a valve (3) and measured by a electromagnetic flowmeter (Hendress+Hausser Picomag II) (4). In the range of the flow rates tested in this work, the accuracy of the instrument is within $\pm 0.5\%$. The electromagnetic flowmeter was chosen for its non-intrusive nature (the flow is not perturbed). This type of flow-

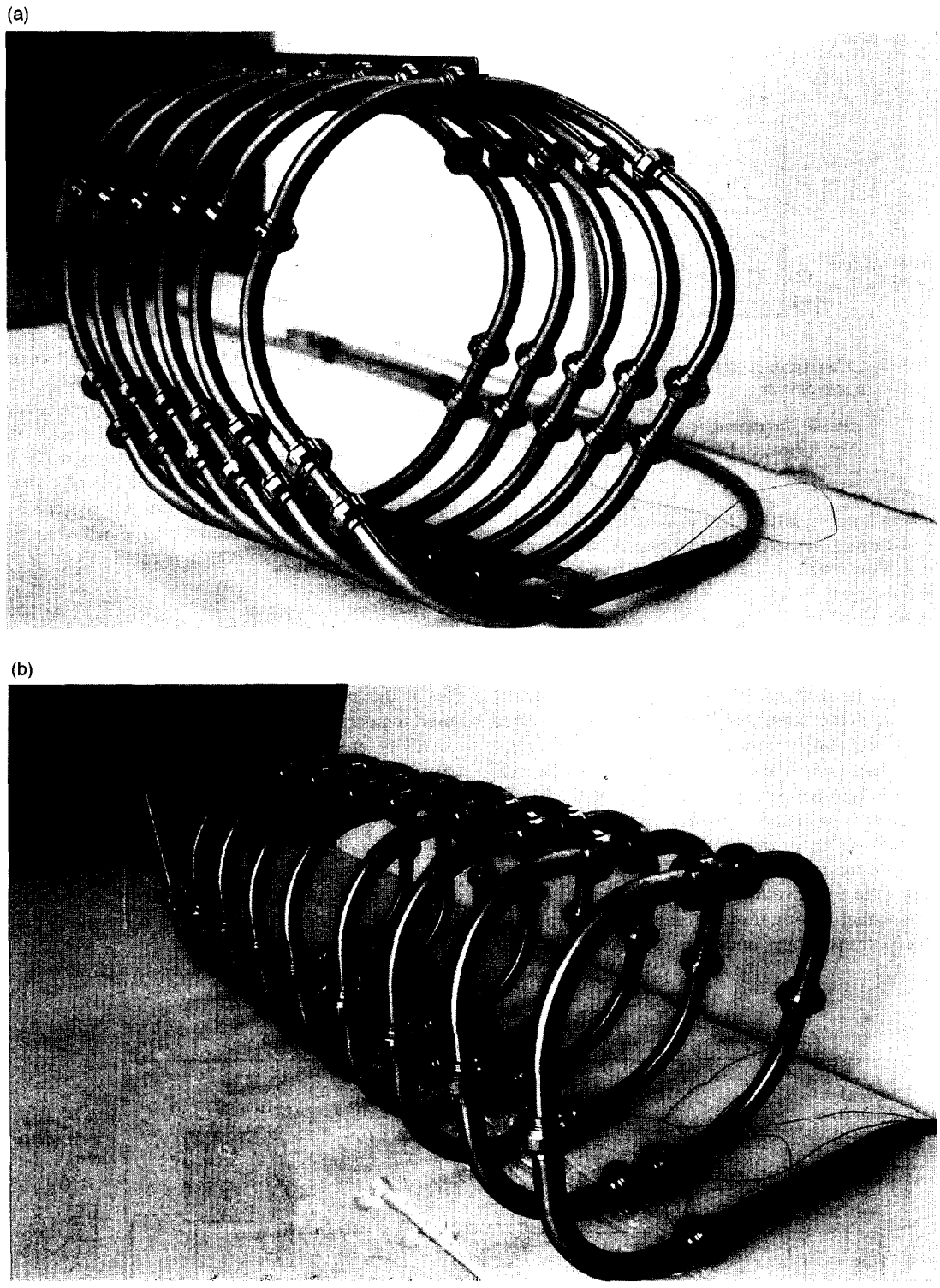

Fig. 2. Photographs of the two coils tested: (a) chaotic coil; (b) helical coil.

meter is also very insensitive to variations in fluid density, viscosity, temperature and flow pressure.

The coil under test is preceded by a 4 m long straight tube (about 170 diameters) in order to obtain a fully developed Poiseuille flow. The fluid is then heated in the coil side of the heat exchanger under test. Before returning to the overhead reservoir, the fluid is cooled to its initial temperature in a compact heat exchanger (5), the coolant fluid of which is the laboratory cold-water network. The temperature of the test fluid (tube side) is controlled by the flow rate of the coolant fluid.

The hot loop, designed to operate with water as

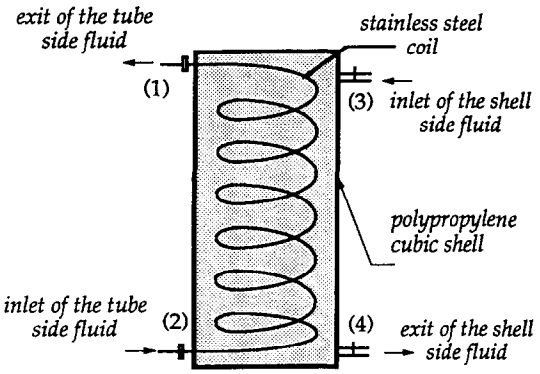

Fig. 3. Heat exchanger test facility.

working fluid, is similar to the cold loop, consisting of an overhead reservoir (6) to damp the temperature fluctuations. The hot fluid is circulated by a centrifugal pump (Grundfos CR4) (7). The flow rate is measured by a bank of three calibrated flow meters with overlapping ranges, arranged in parallel (8). The accuracy of the measurement is within 1.5%. The fluid is then cooled in the shell by the test heat exchanger. Before returning to the overhead reservoir, the fluid is heated to its initial temperature by an Etirex RLE 18 inline electric resistance heater (10). A platinum probe measures the fluid temperature at the exit of the heater, the power of which is regulated by an Etirex PID automatic regulator (model REPN). The precision at the exit of the resistance heater is within $\pm 0.5^{\circ}C$.

Since the two overhead reservoirs damp the temperature fluctuations, the temperatures at the entrance of the heat exchanger under test are obtained within $\pm 0.1^{\circ}C$.

The primary (tube-side) working fluid in the experimental heat exchanger is a viscous non-Newtonian aqueous solution of carboxymethylcellulose (CMC), the shear stress of which is governed by a power law:

$$\tau = k\dot{\gamma}^n \tag{4}$$

where k is the viscosity coefficient, n is the rate index and $\dot{\gamma}$ is the shear rate. CMC has been widely used as a model fluid for the thermal treatment of food liquids. It is opted as the working fluid here in order to investigate the feasibility of chaotic convection for the thermal treatment of food liquids. At the solution concentrations used in these experiments, the non-Newtonian behavior of CMC is very weak and, therefore, at this stage was not taken into analysis. The coefficients k and n were measured with a Weissenberg Rheogoniometer at constant rotation speed; the values obtained are plotted vs temperature in Fig. 5. Both curves show a nonlinear dependence of k and n with temperature. For all temperatures tested, n is less than 1; thus the fluid has pseudoplastic behavior (for a Newtonian fluid, n is a constant equal to 1).

4. RESULTS

Experiments began by measuring axial velocity profiles at the exit from the chaotic coil. We then measured temperature profiles on a tube diameter at the exit from both the chaotic and helical coils. Comparison between the chaotic and helicoidal temperature profiles reveals the effect of chaotic advection. We then proceeded with the assessment of the effect of chaotic advection on global efficiency of the heat exchanger by comparing the heat-exchange efficiency of the two coils. Experiments were run for different flow rates corresponding to Reynolds numbers between 60 and 200.

When a pseudoplastic fluid flows in a circular tube,

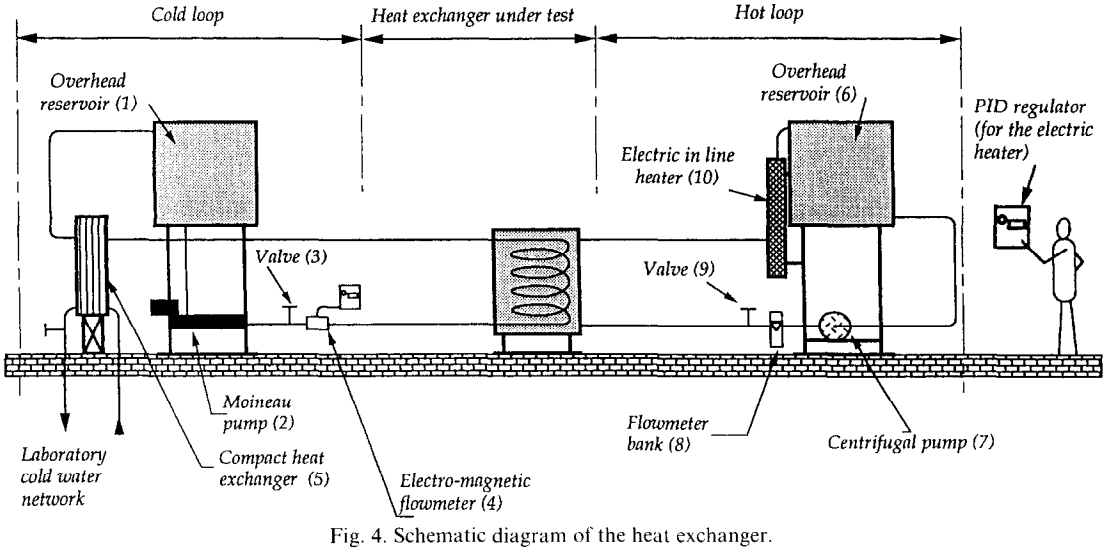

Fig. 4. Schematic diagram of the heat exchanger.

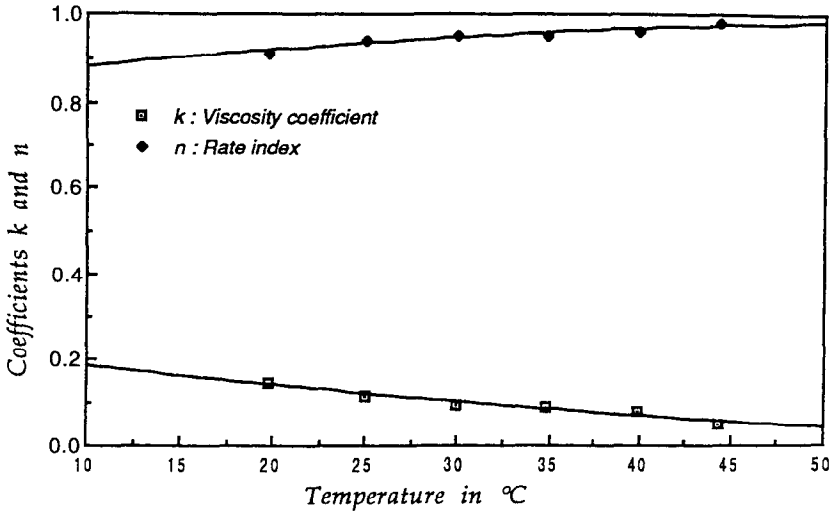

Fig. 5. Variation of the viscosity coefficient k and the rate index n with temperature.

the generalized Reynolds number is calculated from [27]:

$$Re = \left(\frac{4n}{3n+1}\right)^n (8)^{1-n}\left(\frac{(D)^n(V)^{2-n}\rho}{k}\right) \qquad (5)$$

where D is the tube diameter, V is the mean flow velocity and ρ is the fluid density. The advantage of this definition of Reynolds number is that the definition of fanning friction factor f for non-Newtonian fluids remains the same as that of Newtonian fluids; $f = 16/Re$. It is experimentally observed by Metzner and Reed [27] that transition from laminar to turbulent regime occurs at $Re \approx 2100$ for a pipe flow. We present the results below.

4.1. *Flow characterization*

Axial velocity profiles were measured by laser Doppler velocimetry at the exit from the chaotic heat exchanger. In order to measure the velocity profiles, a straight Plexiglas tube with external plane walls was inserted at the exit of the chaotic coil, 200 mm downstream of the last bend. This is the position at which the temperature profiles were also measured. The distance from entrance L, for development of the flow in curved ducts has been found to be 10% longer than that in a straight duct [28]. If we presume that the same length is also necessary for dissipation of Dean roll-cells once they leave a curved duct (and arrive in a straight duct), this length L can be calculated from

$$L = 1.1\left(\frac{DRe}{10}\right). \qquad (6)$$

L was calculated for different experiments reported here and it was found that the distance from the curved pipe exit of the position of velocity measurements was always shorter than L.

Figure 6 shows the axial velocity profiles measured on the symmetry plane of the last bend in the chaotic coil: they are asymmetric parabolic profiles with the maximum shifted to the outer radius of the bend. The shift is a function of the flow Reynolds number; for low Reynolds numbers and low curve angles (90° here), the asymmetry is not very pronounced. However, Dean roll-cells are present, as shown by the conjugate flow visualization and LDV measurements of Castelain [29] in a transparent chaotic twisted duct. Evidently in a helical coil the shift of the velocity maximum toward the outer radius is more pronounced since the curvature effects in bends are additive. Because of the curvature plane switch in the chaotic coil, the curvature effect in each bend is decoupled from that in the neighboring bends. We conclude from the above velocity profiles that in the chaotic coil the flow locally resembles a curved-tube flow with two counter-rotating Dean roll-cells. This conclusion is in agreement with the detailed measurements of le Guer *et al.* [19] in a twisted duct flow.

4.2. *Heat-transfer results*

In all experiments, intake temperatures of the fluid on the tube side and the shell side were regulated at 20 and 46°C, respectively. Shell-side flow was maintained at a fixed flow rate. Experiments were run for 17 flow rates in the tube side corresponding to Reynolds numbers between 60 and 220.

4.2.1. *Temperature profiles. Local analysis.* Temperature profiles were measured on a tube diameter for both helical and chaotic coils. The position of measurements is 200 mm downstream of the last bend exit. Only the temperature profiles that show a significant effect are given here.

Figures 7–9 show fluid temperature profiles measured at the exit from the coil side. For each tube-side flow rate, temperature profiles corresponding to the

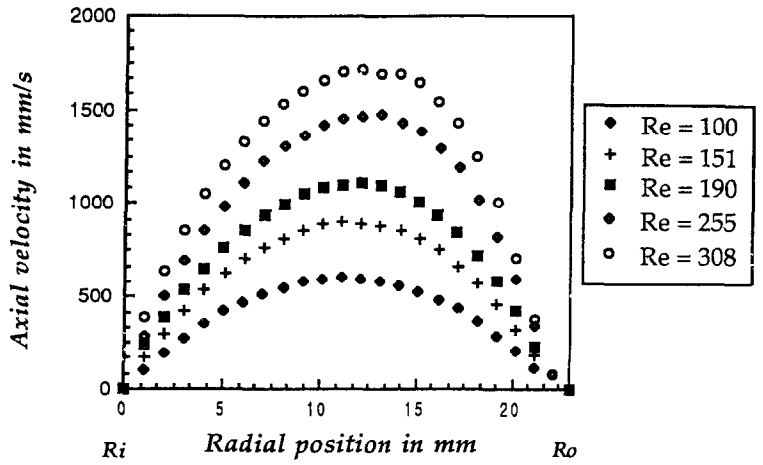

Fig. 6. Axial velocity profiles measured on the symmetry plane of the last bend in the chaotic coil.

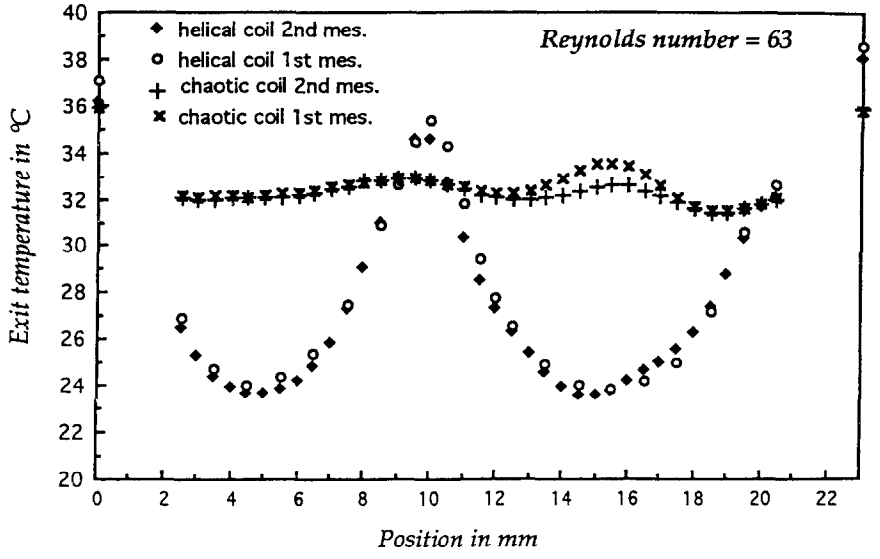

Fig. 7. Temperature profile at the exit of the two coils for Reynolds number 63.

helical and chaotic coils are plotted on the same graph. For the helical coil, profiles are measured perpendicular to the curvature plane of the bends. For the chaotic coil, profiles are measured perpendicular to the curvature plane of the last bend. Profiles labeled "2nd mes." are measurements repeated to verify reproducibility.

For Reynolds numbers between 63 and 97, profiles in the helical coil are "double-U" shaped with the minimum temperatures corresponding to the center of the Dean roll-cells. The maximum temperatures are located close to the wall and in the centerline of the tube. The difference between the maximum and minimum temperatures in a cross-section is more than 12°C. The "overheating" in the center region of the tube is due to the Dean roll-cells, which transport hot fluid particles from the region close to the wall to the centerline and vice versa. However, fluid particles inside the Dean roll-cells are much less heated. During their passage in the coil, particles are trapped between the regular streamlines of the Dean roll-cells and travel on a spiral trajectory, always keeping the same distance from the tube wall. Only a small number of particles can escape from the Dean roll-cells by molecular diffusion. Thus transverse heat transfer inside the vortical structures occurs mainly by conduction. Moreover, the maximum values in the longitudinal velocity profile are located in the center of the Dean roll-cells [1, 27]. Hence, particles situated at these positions have smaller residence time in the coil and are less heated.

For Reynolds numbers greater than 97, the temperature profiles for the helical coil are modified in the neighborbood of the symmetry plane of the Dean roll-cells. The deformation may be due to the appearance of Dean instability. Two additional vortices appear when the Dean number is above a critical value. Called "Dean vortices", they are smaller than the Dean roll-cells and appear on the concave wall of the bends. Therefore they rotate in the opposite

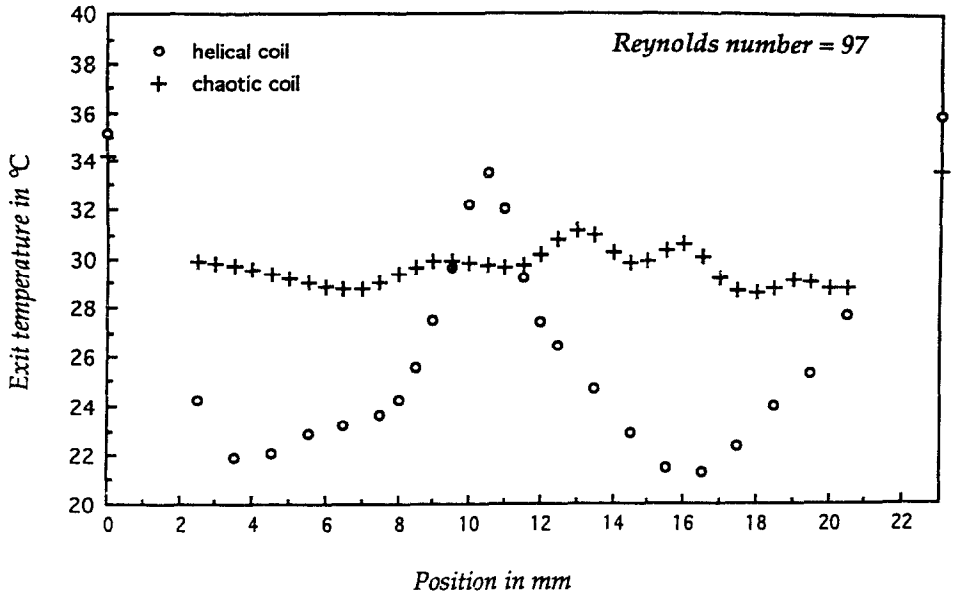

Fig. 8. Temperature profile at the exit of the two coils for Reynolds number 97.

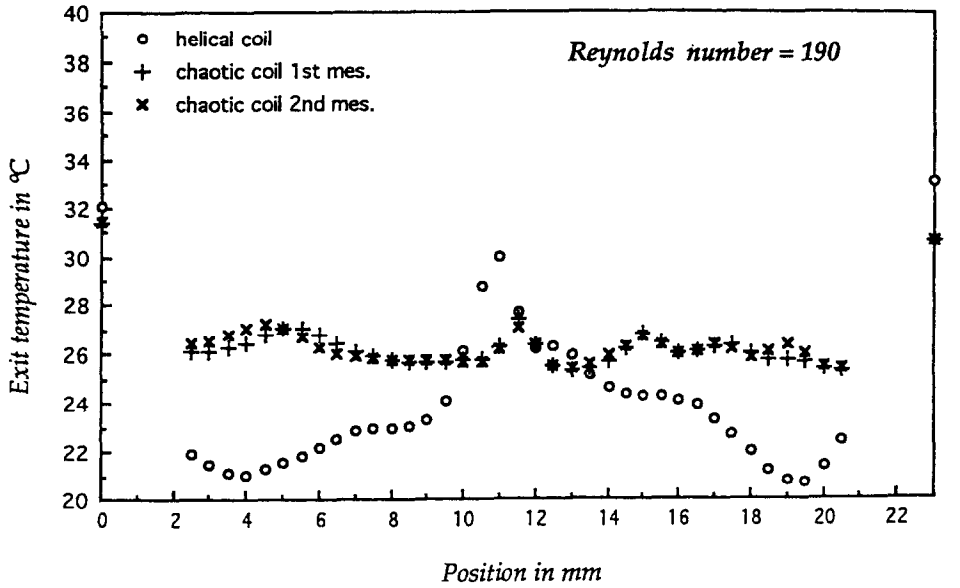

Fig. 9. Temperature profile at the exit of the two coils for Reynolds number 190.

direction to the Dean roll-cells, as shown in Fig. 1. The stagnation point of the Dean roll-cell streamlines is thus pushed away from the concave wall of the bend toward the tube center. The Dean vortices can appear at the origin of the temperature profile deformation, as shown in Fig. 9, corresponding to Reynolds number 190.

Experimental studies confirm the existence of a critical Dean number; however, they do not agree on the critical value. In this study, Dean vortices seem to appear at a lower Dean number than those cited in the literature. This early appearance could occur for various reasons. In a detailed experimental study, Bara *et al.* [25] show that the smaller the Dean number, the greater the development length of Dean vortices. This length is usually given in angular units. Since the primary circuit of the heat exchanger is constituted of 33 90°-angle bends, the helical flow takes nearly 3000° to develop itself. But since the experiments of Bara *et al.* [25] were carried out in a 300° torus, the fluid particles at the exit did not undergo as many rotations as in the present study. It then would be plausible that a larger Dean number is required to reach the threshold of Dean instability.

Another reason for the early appearance of the Dean vortices in the present work could be the nature of the working fluid. The CMC solution used here is mildly pseudoplastic, a property that accelerates the

secondary flow in comparison with a Newtonian fluid [27].

A striking contrast is visible between the temperature profiles at the exit from the helical and chaotic coil. The temperature profiles at the exit of the chaotic coil are almost flat. For Reynolds numbers between 63 and 87, the temperature difference between the core flow and the region close to the wall is less than 4°C and is limited to the zones 2 mm from the wall. The flatness of the temperature profile is affected by chaotic advection. In fact, in this flow regime, while in laminar flow, fluid particles follow chaotic trajectories that make them visit a large number of transverse positions in the tube cross-section. This is in contrast to the helical configuration, in which fluid particles are locked on a regular streamline from entrance to exit from the coil. It is shown numerically [7, 30] by projection of fluid trajectories on the tube cross-section that in chaotic advection fluid particles cross the local transverse streamlines, while in the helical configuration transverse streamlines are barriers to free particle movement.

Superposed on the globally flat temperature profiles of chaotic coil, a small-amplitude spatial wave-form is observed. When the Reynolds number was increased more waves appeared, but in no cases did their amplitude exceed 3°C. From the present exit measurements it is difficult to decide on the cause of these waveforms. One possible reason is the existence in the flow of KAM tori, which are closed stream tubes across which no fluid particle can pass. Thus if a KAM torus initially contains hot fluid particles, they do not transfer heat to cooler fluid particles and, thus, at the exit are hotter than their environment. The formation and behavior of KAM tori in the chaotic coil was numerically demonstrated in previous work [30].

The flow in the chaotic coil is three-dimensional. The effect of chaotic advection is verified by measurement of the temperature profile on a tube diameter perpendicular to that in Figs 7–9. In Fig. 10 temperature profiles along a horizontal and a vertical diameter of the chaotic coil are superposed on the temperature profile on a horizontal diameter of a helical coil. The Reynolds number for the three measurements is 63. The similar form of the chaotic temperature profiles (horizontal and vertical) is readily discernible, suggesting that the temperature profiles on other diameters will behave similarly.

In summary, the main difference between the helical and the chaotic coils can be qualitatively described from the local temperature measurements. In the helical coil the Dean roll-cells transport hot particles from the neighborhood of the wall to the center of the tube and vice versa. However, particles trapped at the center of the Dean roll-cells are prevented from approaching the hot wall. Consequently the centerline of the tube is overheated and the center of the Dean roll-cells are not heated enough. Heating in the helical coil is thus nonhomogeneous. The Dean roll-cells are also locally present in the bends of the chaotic coil, but each curvature-plane switch reorients the centrifugal force, so the Dean roll-cells of the previous bend van-

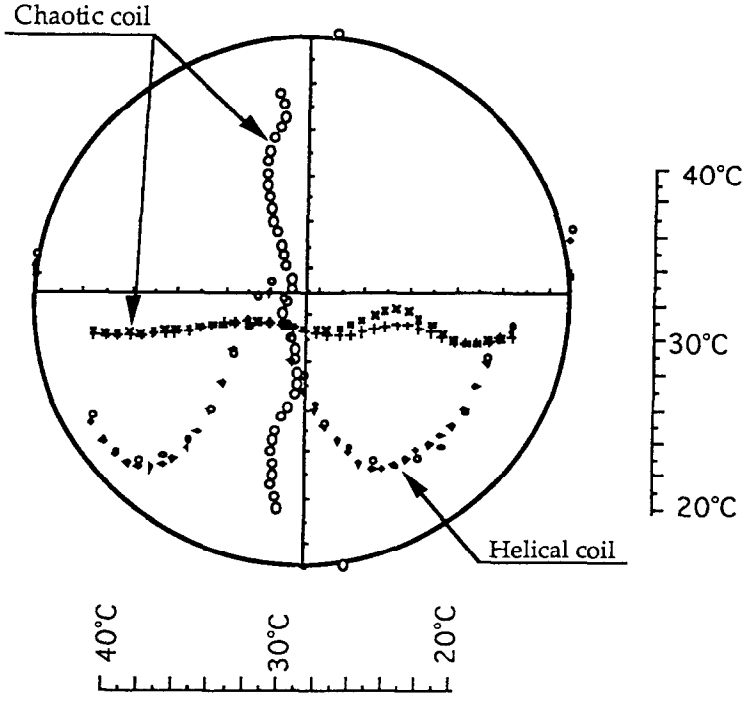

Fig. 10. Temperature profiles for the chaotic coil measured in the curvature plane of the last bend and in a plane perpendicular to the latter. Temperature profiles for the helical coil measured in the plane perpendicular to the curvature plane.

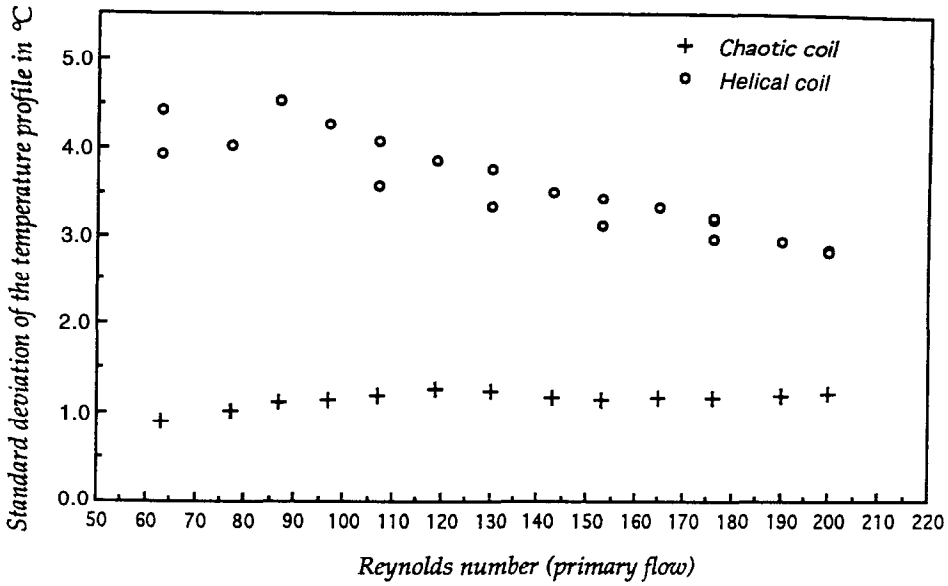

Fig. 11. Standard deviation of the temperature profiles vs the Reynolds number.

ish and reappear in a plane perpendicular to the previous plane. Fluid particles that were trapped in the Dean roll-cells of the previous bend are released and mixed in the Dean roll-cells of the next bend, so that more particles can visit hot regions close to the walls. The consequence of these phenomena is the homogenization of heating in chaotic flow.

Acharya *et al.* [8] have demonstrated the feasibility of heat-transfer enhancement by chaotic mixing. They have solved the problem numerically by using the analytical flow field obtained by Dean [21, 22]. The energy equation, though linear, is solved numerically, using Dean's velocity field, to give the temperature distributions and heat-transfer characteristics. They found also that in the alternating axis coil, the temperature field becomes flatter than in helical coil.

Standard deviation of the profiles. Here we examine the standard deviation of the temperature distribution in order to give a rough quantitative criterion for heating homogeneity. The standard deviation, which indicates the scattering of the temperatures around their mean value, gives sufficient insight into the problem: the smaller the standard deviation, the more homogeneous the heating.

Figure 11 plots the standard deviation of the temperature profiles vs the Reynolds number of the tube-side flow. The values corresponding to the chaotic coil, of the order of 1°C, do not vary significantly with Reynolds number: the homogeneity of heating seems to be independent of the Reynolds number. On the other hand, for the regular flow in the helical coil, the values decrease from 4.5°C to 3°C: increasing the Reynolds number seems to homogenize heating.

These curves confirm that in chaotic flow, mixing in the cross-section of the tube is almost independent of the dynamics of the flow; instead, the chaotic behavior of the particles is inherent in the flow topology. On the contrary, in the regular flow, the strength of the secondary flow (characterized by the Reynolds or Dean number) plays a leading role in the mixing process.

4.2.2. *Effect of chaotic advection on global heat transfer.* A series of experiments was carried out to examine the effect of chaotic advection on global heat transfer in the coils by assessing the efficiency of heat exchange in the chaotic and helical configurations. This requires measuring the bulk fluid temperatures at the entrance and exit of both the coils and the shell. Since important temperature variations are detected in the tube cross-section, as shown earlier, we used the mixing device described below to obtain a mixed mean fluid or bulk temperature.

Measurement of the bulk temperature. The exit temperature of the tube-side fluid was measured using a SMX Sulzer static mixer. The model chosen has five elements. In order to verify the homogeneity of the temperature in the cross-section, we measured temperature profiles downstream of the mixer. The device used for this operation (see Fig. 12) consists of two thermocouples. The first is fixed in the center of the tube and measures the bulk temperature. This temperature is then compared to the local temperatures on the profile. Local temperatures are measured by a second thermocouple that is displaced by the micrometric traversing mechanism shown in Fig. 12.

Figure 13 shows three temperature profiles measured for different Reynolds numbers. The straight lines indicate the values of bulk fluid temperature measured by the fixed thermocouple and "o" symbols represent local temperatures in the tube cross-section, downstream of the static mixer, measured by the traversing mechanism. Temperature profiles are very flat; the difference between local and bulk temperatures is less than 0.25°C. Therefore, we can consider the fluid

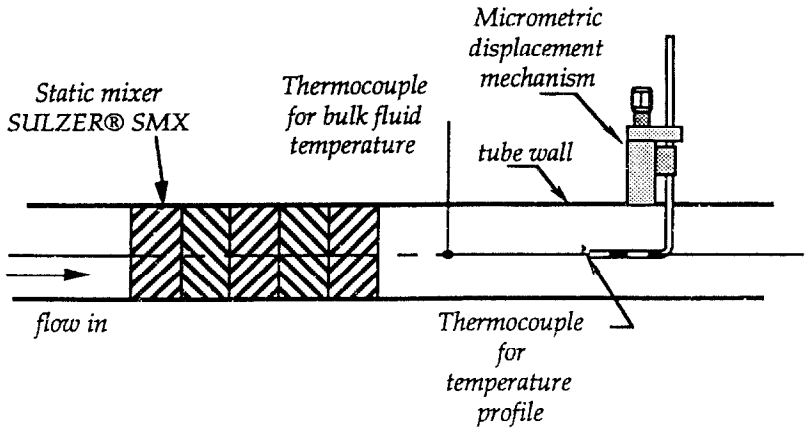

Fig. 12. Mixing temperature device.

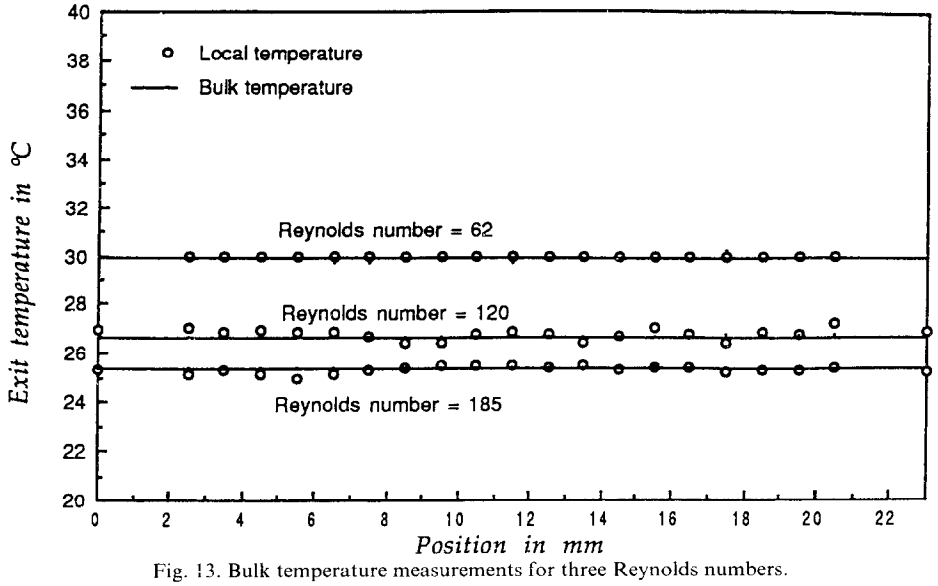

Fig. 13. Bulk temperature measurements for three Reynolds numbers.

temperature measured at the center of the tube as the bulk fluid temperature with satisfactory accuracy.

Determination of the efficiency of the heat exchanger. The physical properties of the tube side fluid are calculated for its average temperature in the heat exchanger, determined as

$$T_{av} = \frac{T_{it} + T_{ot}}{2} \tag{7}$$

where the subscript i refers to the intake, o to the exit and t to the tube-side fluid. The thermal energy received by the tube side fluid is calculated from

$$\phi_t = \rho_t Q_t C_{p_t}(T_{ot} - T_{it}). \tag{8}$$

The following expression defines the efficiency of a heat exchanger:

$$\varepsilon = \frac{\phi_t}{(\rho Q C_p)_{min}(T_{is} - T_{it})}. \tag{9}$$

For all experiments in the present work, the term $(\rho Q C_p)_{min}$ corresponds to the tube-side fluid. Thus calculating the efficiency of the heat exchanger reduces to calculating the ratio of two temperature differences:

$$\varepsilon = \frac{T_{ot} - T_{it}}{T_{is} - T_{it}}. \tag{10}$$

Thermal equilibrium criterion. For each experiment, a criterion for thermal equilibrium was verified before recording the measurements: measurements were taken when the heat balance was within 5%. This takes into account the heat losses from the exchange among the six faces of the shell and the surrounding air.

To check the heat balance, we compare the primary and secondary heat fluxes. The secondary (shell-side) heat flux is determined as

$$\phi_s = \rho_s Q_s C_{p_s}(T_{os} - T_{is}) \tag{11}$$

where the subscript s refers to the shell-side fluid. Since

the shell side fluid is the hotter one, the secondary heat flux is negative.

The criterion for thermal equilibrium-state is then written as

$$\frac{\phi_t + \phi_s}{\phi_t} \leqslant 0.05. \quad (12)$$

The term on the left-hand side of the above criterion is plotted vs Reynolds number in Fig. 14. The graph represents the thermal equilibrium for different experiments in the present work. The values scatter within $\pm 5\%$, but most of them are contained between $\pm 2.5\%$.

Efficiency of the heat exchanger. Figure 15 plots the efficiency of the heat exchanger vs Reynolds number for the two coil configurations, "+" symbols correspond to the chaotic coil and "o" symbols to the helical coil.

Vertical bars indicate the uncertainties of the values. The uncertainty interval for ε is due to the errors in measuring the temperatures T_{ot}, T_{is} and T_{it}. As mentioned in Section 3, 80 μm thermocouples were used. The uncertainties for temperature have been estimated to be equal to 0.1°C. Using the method described by Kline and McClintock [31] and Moffat [32], we have calculated the relative uncertainty interval for ε. They vary from 1.2% for high values of ε to 2.5% for lower values. As can be seen on Fig. 15 this results to absolute uncertainty intervals approximately constant and of the order of 0.006.

The points follow two separate curves: the values corresponding to the chaotic coil are always higher than those for the helical coil. The efficiency of the chaotic heat exchanger is thus greater than that of the helical heat exchanger.

In the chaotic flow, the cold fluid is no longer contained in the cold region. The location of the Dean roll-cells changes from one bend to the next. Thus, the fluid trapped in the Dean roll-cells is released at the change of the curvature plane. More cold particles of fluid thus visit hot regions close to the wall and global heat transfer is therefore improved.

Figure 16 plots the efficiency enhancement, defined by the relative increase of the efficiency of the chaotic heat exchanger over the helical heat exchanger, versus the Reynolds number. The points follow a constant plateau (around 27%) for Reynolds numbers up to 90 and then the efficiency enhancement decreases with Reynolds number. Its lowest value is 13%, which corresponds to $Re = 220$, the largest Reynolds number considered here. Measurement of the friction coefficient at these low Reynolds numbers revealed no significant difference between chaotic and helical coils [9].

Heating in chaotic advection is more advantageous at lower Reynolds numbers, as shown in Fig. 16. Indeed, in the chaotic flow, the complex behavior of the pathlines is independent of the dynamics of the flow and is instead due to kinematic effects. However, mixing in regular flow is directly governed by the dynamics of the flow. In chaotic flow, better mixing does not require higher Reynolds number if the secondary flow has reached an invariant state.

5. CONCLUSIONS AND DISCUSSION

A new geometry for the tube coil in the shell-and-tube heat exchanger is presented, inspired by previous work of the authors on the generation of the spatially chaotic regime in dynamical systems. The basic

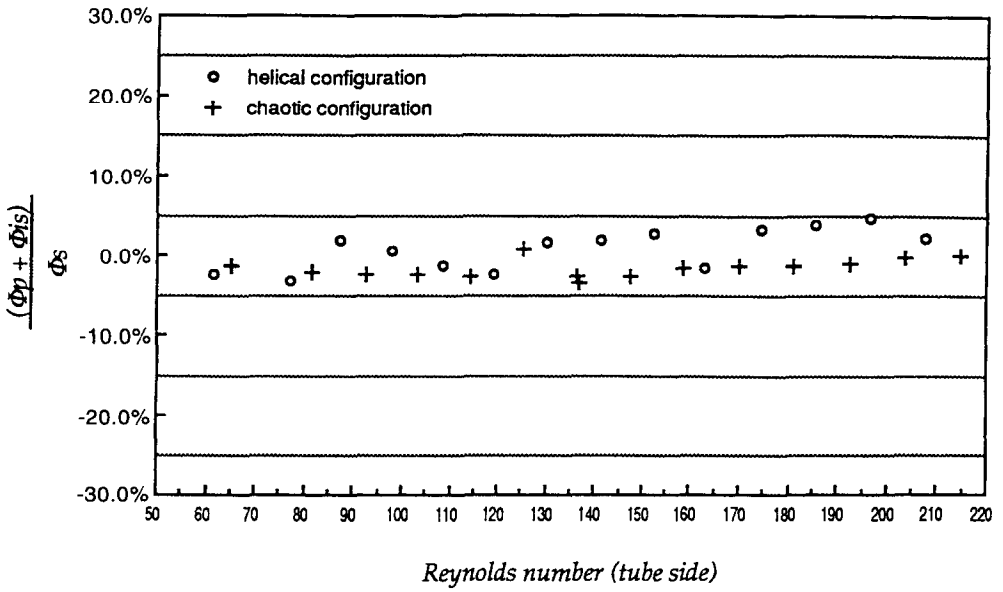

Fig. 14. Thermal equilibrium criterion vs Reynolds number.

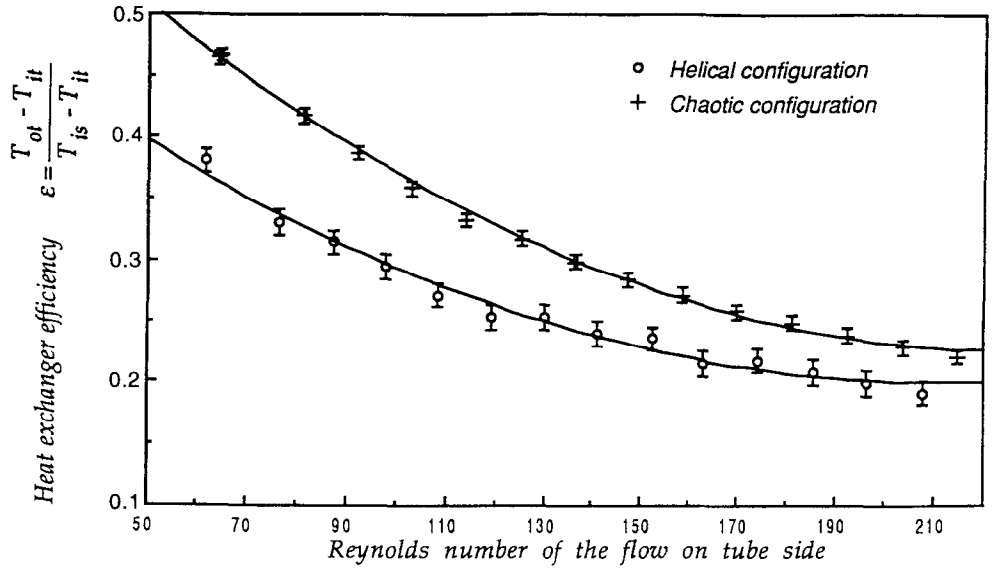

Fig. 15. Efficiency of chaotic and helical heat exchangers vs Reynolds number.

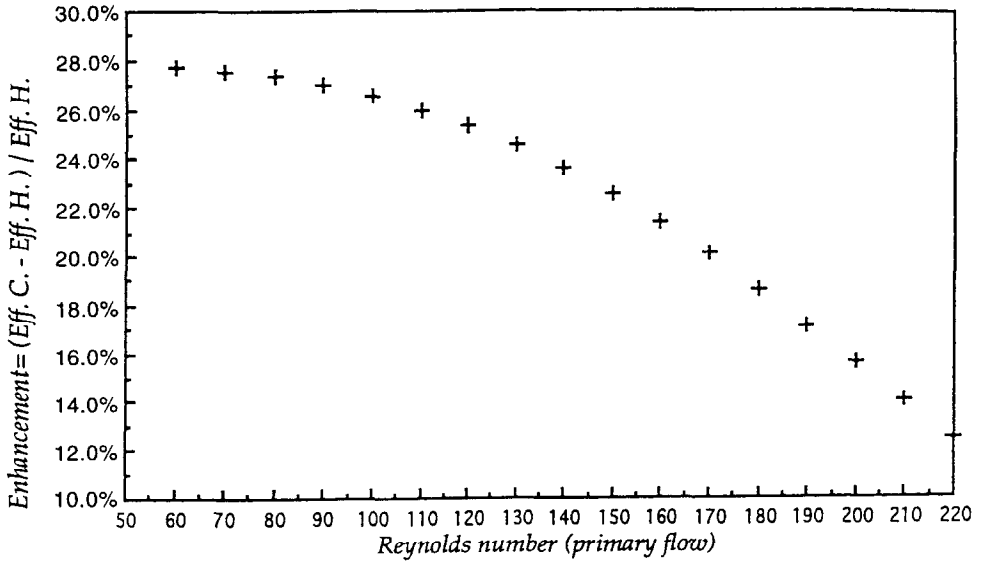

Fig. 16. Relative enhancement of chaotic heat exchanger efficiency over that of helical heat exchanger.

geometry of the tube coil is constituted from an ensemble of quarter-circle curved tubes or bends. The curvature plane of each bend makes a 90° angle with those of neighboring bends. Dean roll-cells generated in the bends are the building blocks of a stretching and folding process that increases mixing in the fluid, thus enhancing heat transfer.

A chaotic shell-and-tube heat exchanger was designed on the basis of this geometry. The basic elements (bends) of the chaotic coil were reassembled to build a helical tube, which was in turn used to construct a helical shell-and-tube heat exchanger. The performance of the two heat exchangers was studied on a heat-exchanger test facility specifically designed for this purpose. The effect of chaotic advection in the chaotic heat exchanger on temperature uniformity, as well as on the overall efficiency of the heat exchanger, was assessed.

It was found that Dean roll-cells generated in the curved tubes are locally similar in chaotic and helical heat exchangers. However, their effects on convective heat transfer between the tube wall and fluid are quite different, even opposite. In the chaotic coil, the Dean roll-cells smear temperature differences in the tube cross-section and, therefore, render it uniform. On the contrary, in the helical or regular coil, they generate confined regions in the tube cross-section in which fluid particles trapped inside Dean roll-cells stay trap-

ped from the entrance to the exit of the helical coil; they can escape these closed zones only by diffusion. This segregation causes zones of overheating separated by regions of no heating and hence a non-uniform temperature in the tube cross-section.

The flatter temperature distribution in the chaotic coil is attributed to the chaotic trajectories of fluid particles due to the generation of the chaotic advection regime. This phenomenon contributes also to the enhancement of the global efficiency of the chaotic heat exchanger. The relative enhancement of the chaotic heat exchanger, measured for tube Reynolds numbers ranging between 60 and 200, was up to 28%. This increase occurred at Reynolds numbers as low as 60, where most enhancement techniques have encountered difficulties. The great efficiency of the chaotic heat exchanger makes it an attractive device for heating very viscous or fragile Newtonian or non-Newtonian fluids. As a general rule, it can be stated that chaotic advection always improves the already high efficiency of helical coils.

Previous studies on helical coils have shown that the secondary flow, though regular, improves global heat transfer compared with a straight tube, for the same heat-transfer surface area. The inner Nusselt number of a helical coil is higher than that of a straight tube [1–3]. Kalb and Seader [33] showed that the ratio of the relative enhancement of the Nusselt number to the relative augmentation of the friction factor increases with the Prandtl number of the fluid. This ratio lies between 1.5 and 2 for a Prandtl number of 7. Indeed, in convective heat transfer, mixing is most important when conduction is weak compared to advection. Therefore, one can expect the chaotic heat exchanger to be more advantageous than the helical heat exchanger for higher Prandtl numbers, a result proved numerically by Acharya *et al.* [8].

In coiled tubes periferally averaged Nusselt number is found to undergo spatial oscillations before reaching an axially invariant fully developed value [34]. Acharya *et al.* [34] showed that for unit Prandtl number the Nusselt number goes through a minimum when the eccentricity (due to the development of the secondary flow) of the isotherms is of the same order that the boundary layer thickness developed on the tube walls. They also showed that the Nusselt number reaches a maximum value farther downstream and then begins to decrease again. The passage on maximum occurs at axial distance from the tube entrance Z_{max} which scales as

$$Z_{max}\delta^{1/4}Re^{-1/2} \approx 0.85. \quad (13)$$

Z_{max} is approximately the axial distance necessary for a fluid particle at the tube center to reach the wall. Eventually the entrance length Z_e is defined as the distance at which the Nusselt number becomes axially invariant. The authors have found that $Z_e \approx 2Z_{max}$ and that it is a function of the Prandtl number. For fluids with $Pr > 1$ the curve of the Nusselt number shows more than one oscillation. We have calculated Z_e for the experimental cases reported here, using the estimation (13). It is found that even for the lowest Reynolds number the entrance length Z_e is longer than the bend length. It implies that in the chaotic configuration the Nusselt number never reaches its fully developed asymptotic value. On the contrary, in the helically coiled configuration the tube length is more than 23 times the entrance length calculated for $Pr = 1$. The Prandtl number for CMC used in this work is 30, which is evidently higher than 1. However, it can be presumed that the entrance length corresponding to $Pr = 30$ should be at most one order of magnitude longer than that of $Pr = 1$ and, therefore, the helical tube length is long enough to provide fully developed regime. The temperature profiles (Figs 7–9) somehow show this.

The non-establishment of fully developed value of Nusselt number, in fact causes an underestimation effect of the heat transfer enhancement by chaotic advection. In other words one can consider the values of efficiency gain reported here as a lower bound for efficiency enhancement by chaotic advection.

Mixing and heat transfer by chaotic advection can also be sensitive to the protocol of rotation of the curvature plane. Acharya *et al.* [8] studied heat-transfer enhancement in a coil by chaotic advection. In their case, the secondary flow was already established by a preconditioner helical coil before the flow entered the test coil, which was also followed by a post-conditioner coil. The test chaotic coil, made of 180° bends, was immersed in a constant-temperature bath. Experiments were run for Reynolds numbers ranging from 3000 to 10 000. The authors observed an increase of 6–8% of the inner heat-transfer coefficient at high Reynolds numbers. The corresponding pressure drop was 1.5–2.5%.

The protocol of curvature plane switch in Acharya *et al.* [8] was slightly different from that of this work: there, half circle elements are repeated with 90° angle between every two adjacent element. In this configuration the bent elements occupy two planes in the three-dimensional space. The authors numerically show that chaotic trajectories are produced in this configuration. We recall that in the work presented here, all bends rotate 90° with respect to their neighboring bends and are placed in three perpendicular planes in space.

The difference between the enhancement observed in this work (13–28%) and that of Acharya *et al.* (6–8%) is due to the low Reynolds number and high Prandtl number of the CMC fluid used here. The low Reynolds number amplifies the marginal mixing effect of chaotic advection. The Prandtl number also has the same effect as the viscous effect and is enlarged over the thermal diffusive effect*.

* We are indebted to one of the referees for this comment.

REFERENCES

1. Shah, R. K. and Joshi, S. D., Convective heat transfer in curved ducts. *Handbook of Single-Phase Convective Heat Transfer*. Wiley, New York, 1987, 5.1–5.46.
2. Mori, Y. and Nakayama, W., Study on forced convective heat transfer in curved pipes (1st report, laminar region). *International Journal of Heat and Mass Transfer*, 1965, **8**, 67–82.
3. Dravid, A. N., Smith, K. A., Merrill, E. W. and Brian, P. L. T., Effect of secondary fluid motion on laminar heat transfer in helically coiled tubes. *AIChE Journal*, 1971, **17**(5), 1114–1122.
4. Akiyama, M. and Cheng, K. C., Laminar forced convection heat transfer in curved pipes with uniform wall temperature. *International Journal of Heat and Mass Transfer*, 1972, **15**, 1426–1431.
5. Patankar, S. V., Pratap, V. S. and Spalding, D. B., Prediction of laminar flow and heat transfer in helically coiled pipes. *Journal of Fluid Mechanics*, 1974, **62**(3), 539–551.
6. Raju, K. K. and Rathna, S. L., Heat transfer for the flow of a power law fluid in a curved pipe. *Journal of Indian Institute of Science*, 1970, **52**, 34–37.
7. Jones, S. W., Thomas, O. M. and Aref, H., Chaotic advection by laminar flow in twisted pipe. *Journal of Fluid Mechanics*, 1989, **209**, 335–357.
8. Acharya, N., Sen, M. and Chang, H. C., Heat transfer enhancement in coiled tubes by chaotic advection. *International Journal of Heat and Mass Transfer*, 1992, **35**(10), 2475–2489.
9. Peerhossaini, H., Castelain, C. and Le Guer, Y., Heat exchanger design based on chaotic advection. *Experimental and Thermal and Fluid Science*, 1993, **7**, 333–334.
10. Aref, H., Stirring by chaotic advection. *Journal of Fluid Mechanics*, 1984, **143**, 1–21.
11. Chaiken, J., Tabor, C. K. and Tan, Q. M., Lagrangian turbulence and spatial complexity in a stokes flow. *Physical Fluids*, 1987, **30**, 687–694.
12. Jones, S. W. and Aref, H., Chaotic advection in a pulsed source-sink system. *Physics Fluids*, 1990, **31**, 469–485.
13. Ghosh, S., Chang, H. C. and Sen, M., Heat transfer enhancement due to slender recirculation and chaotic transport between counter-rotating eccentric cylinders. *Journal of Fluid Mechanics*, 1992, **238**, 119–154.
14. Saatdjian, E., Midoux, N. and André, J. C., On the solution of Stokes equations between confocal ellipses. *Physical Fluids*, 1994, **6**, 3833–3846.
15. Saatdjian, E., Midoux, N., Gastou-Chassaing, M. I., Lepervost, J. C. and André, J. C., Chaotic mixing and heat transfer between confocal ellipses: experimental and numerical results. *Physical Fluids*, 1996, **8**, 677–691.
16. Arnold, V. I., Sur la topologie des écoulements stationnaires des fluides parfaits. *C. R. Acad. Sci. Paris*, 1965, **261**, 17–20.
17. Khakhar, D. V., Franjione, J. G. and Ottino, J. M., A case study of chaotic mixing in deterministic flows: the partitioned-pipe mixer. *Chemical Engineering Science*, 1987, **42**(12), 2909–2926.
18. Le Guer, Y. and Peerhossaini, H., Order breaking in Dean flow. *Physical Fluids*, 1991, **A3**(5), 1029–1032.
19. Le Guer, Y., Castelain, C. and Peerhossaini, H., Experimental study of chaotic advection regime in a twisted duct flow. *Journal of Fluid Mechanics*, 1995 (submitted).
20. Doherty, M. F. and Ottino, J. M., Chaos in deterministic systems: strange attractors, turbulence and applications in chemical engineering. *Chemical Engineering Science*, 1988, **43**(2), 139–183.
21. Dean, W. R., Note on the motion of fluid in a curved pipe. *Philosophical Magazine Journal of Science*, 1927, **4** (7th series), 208–223.
22. Dean, W. R., The stream-line motion of fluid in a curved pipe. *Philosophical Magazine Journal of Science*, 1928, **5**, 673–695.
23. Eustice, J., Experiments on streamline motion in curved pipes. *Proceedings of the Royal Society*, 1911, **A85**, 119.
24. Berger, B. A., Talbot, L. and Yao, L. S., Flow in curved pipes. *Annual Review of Fluid Mechanics*, 1983, **15**, 461–512.
25. Bara, B., Nandakumar, K. and Masliyah, J. H., An experimental and numerical study of the Dean problem: flow development towards two-dimensional multiple solutions. *Journal of Fluid Mechanics*, 1992, **244**, 339–376.
26. Chang, H. C. and Sen, M., Application of chaotic advection to heat transfer. *Chaos, Solitons and Fractals*, 1994, **4**, 955–976.
27. Metzner, A. B. and Reed, J. C., Flow of non-Newtonian fluids: correction of the laminar transition and turbulent flow regions. *AIChE Journal*, 1955, **1**, 434.
28. Yao, L. S. and Berger, S. A., The three-dimensional boundary layer in the entry region of curved pipes with finite curvature ratio. *Physical Fluids*, 1988, **31**, 486–494.
29. Castelain, C., Etude expérimentale de la dynamique des fluids et des transferts thermiques dans un écoulement de Dean alterné en régime d'advection chaotique. Ph. D. thesis, University of Nantes, France, 1995.
30. Le Guer, Y., Etude des phénomènes de transport en régime d'advection chaotique dans un écoulement ouvert. Ph. D. thesis, University of Nantes, France, 1993.
31. Kline, S. J. and McClintock, F. A., Describing uncertainties in single-sample experiments. *Mechanical Engineering*, 1953, **75**, 3–8.
32. Moffat, R. J., Describing the uncertainties in experimental results. *Experimental Thermal and Fluid Science*, 1988, **1**, 3–17.
33. Kalb, C. E. and Seader, J. D., Fully developed viscous flow heat transfer in curved circular tubes with uniform wall temperature. *AIChE Journal*, 1974, **20**(2), 340–346.
34. Acharya, N., Sen, M. and Chang, H. C., Thermal entrance length and Nusselt numbers in coiled tubes. *International Journal of Heat and Mass Transfer*, 1994, **10**, 336–340.